Finite-range corrections near a Feshbach resonance and their role in the Efimov effect

P. Dyke, S. E. Pollack, and R. G. Hulet

Department of Physics and Astronomy and Rice Quantum Institute, Rice University, Houston, Texas 77005, USA

(Received 1 February 2013; published 30 August 2013)

We have measured the binding energy of ^{7}Li Feshbach molecules deep into the nonuniversal regime by associating atoms in a Bose-Einstein condensate with a modulated magnetic field. We extract the scattering length from these measurements, correcting for nonuniversal short-range effects using the field-dependent effective range. With this more precise determination of the Feshbach resonance parameters we reanalyze our previous data on the location of atom loss features produced by the Efimov effect [Pollack *et al.*, Science **326**, 1683 (2009)]. We find the measured locations of the three- and four-body Efimov features to be consistent with universal theory at the 20%–30% level.

DOI: 10.1103/PhysRevA.88.023625 PACS number(s): 03.75.Kk, 03.75.Lm, 47.37.+q, 71.23.−k

Efimov showed more than 40 years ago that three particles interacting via resonant two-body interactions could form an infinite series of three-body bound states as the two-body s-wave scattering length a was varied [1]. In the limit of zero-range interactions, the ratios of scattering lengths corresponding to the appearance of each bound state were predicted to be a universal constant, equal to approximately 22.7. The only definitive observations of the Efimov effect have been in ultracold atoms, where the ability to tune a via a Feshbach resonance [2,3] has proven to be essential. Since the first evidence for Efimov trimers was obtained in ultracold Cs [4], experiments have revealed both three- and four-body Efimov states in several atomic species. Although the Efimov effect has now been confirmed, several open questions remain, including a full understanding of the role of nonuniversal finite-range effects. Accurate comparisons with theory require that these nonuniversal contributions be quantitatively determined and incorporated.

We previously characterized the $F = 1, m_F = 1$ Feshbach resonance in ^{7}Li, which is located at approximately 738 G, by extracting a from the measured size of trapped Bose-Einstein condensates (BEC) assuming a mean-field Thomas-Fermi density distribution [5,6]. These data were fit to obtain $a(B)$, the function giving a versus magnetic field, which was used to assign values of a to Efimov features observed in the rate of inelastic three- and four-body loss of trapped atoms [5]. More recently, two groups have characterized the same Feshbach resonance by directly measuring the binding energy, E_b, of the weakly bound dimers on the $a > 0$ side of the Feshbach resonance [7–9]. These measurements disagree with our previous measurements based on BEC size. The disagreement in the parameters characterizing the Feshbach parameters is sufficiently large to affect the comparison of the measured Efimov features with universal theory.

In this paper, we report measurements of E_b, which we fit to obtain $a(B)$. The measurement of E_b has fewer systematic uncertainties than the BEC size measurement, which is affected at large scattering length by beyond mean-field effects and by anharmonic contributions to the trapping potential. The extraction of a from E_b can therefore be more accurate, and unlike the condensate size measurement, E_b is related to a for both thermal gases and condensates. We have measured E_b far enough from the Feshbach resonance that E_b no longer depends quadratically on the detuning of B from resonance, as it would in the universal regime [2,3]. We show that a commonly adopted correction for nonuniversal finite-range effects, which depends on a single value for the effective range, does not fit the data as satisfactorily as more complex two-channel models [10,11] that accommodate a field-dependent effective range, or a model that incorporates an explicit calculation of the effective range. We employ the latter strategy to produce an improved $a(B)$ function to reanalyze our three- and four-body loss data to obtain more accurate locations of the Efimov features.

Our experimental methods for producing BECs and ultracold gases of ^{7}Li have been described in detail previously [6]. Atoms in the $|F = 1, m_F = 1\rangle$ state are confined in an optical trap formed from a single focused laser beam with wavelength of 1.06 μm. A bias magnetic field, directed along the trap axis, is used to tune a via the Feshbach resonance. For the data presented here the axial and radial trapping frequencies are 4.7 and 255 Hz, respectively. We adjust the magnetic field to give $a \sim 200\, a_0$, where a_0 is the Bohr radius, and use forced evaporation to produce either ultracold thermal clouds with temperatures of $\sim 3\,\mu$K, or condensates with a condensate fraction that we estimate is greater than 85%. We then adiabatically ramp the field to the desired value and employ *in situ* imaging, either polarization phase contrast [12] when the density is high, or absorption imaging in less dense clouds.

Atoms are associated into Feshbach molecules by resonantly oscillating the magnetic field at a frequency $h\nu_{\rm mod} = E_b + E_{\rm kin}$, where E_b is taken to be positive for a bound state, and $E_{\rm kin}$ is the relative kinetic energy of the atom pair [13,14]. The weakly bound dimers formed in this way are lost from the trap through collisional relaxation, presumably into deeply bound vibrational levels [13]. This technique has been used in studies of both homonuclear [10,13,15] and heteronuclear [16–18] Feshbach resonances, in addition to the specific hyperfine state of ^{7}Li studied here [7–9].

The oscillating field is produced by a set of auxiliary coils that are coaxial with the bias coils producing the Feshbach field. The amplitude of this field ranges from 0.1 to 0.6 G and the duration of modulation ranges from 25 to 500 ms depending on magnetic field. The number of remaining atoms are measured as a function of the frequency of the oscillating

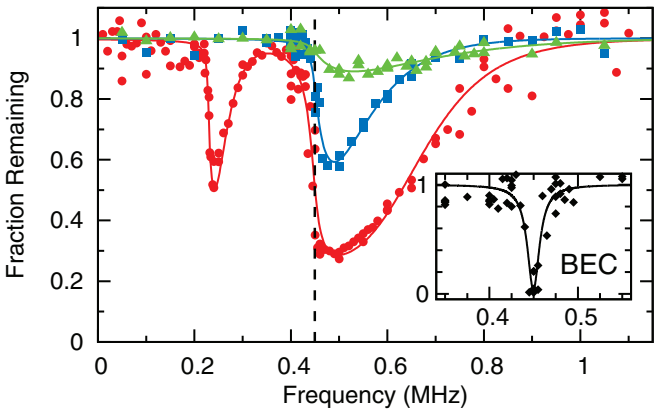

FIG. 1. (Color online) Magneto-association induced loss at $B = 734.5$ G, where $a \simeq 1100\,a_0$. The main plot shows loss spectra for thermal gases with the following modulation amplitudes and approximate temperatures: green (triangles) 0.57 G/10 μK; blue (squares) 0.14 G/3 μK; and red (circles) 0.57 G/3 μK. The solid curves are fits to Lorentzians convolved with thermal Boltzmann distributions. For the 0.57 G/3 μK data the lower frequency resonance is a subharmonic response, while the primary resonance is thermally broadened by strong modulation. The inset (black diamonds) corresponds to a BEC with a modulation amplitude of 0.14 G. The solid black line is a Lorentzian fit to the condensate resonance and the vertical dashed line in the main figure is the resonance location $E_b/h = 450$ kHz found from this fit.

field. We find that in the case of a BEC the loss spectra are fit well by a Lorentzian lineshape, while for a thermal gas, we fit the loss spectra to a Lorentzian convolved with a thermal Boltzmann distribution [7,14,18].

Figure 1 shows characteristic loss spectra at 734.5 G (where $a \simeq 1100\,a_0$) for several different temperatures and modulation amplitudes. The Lorentzian component fits to a linewidth of 8 kHz, which provides a lower bound on the lifetime of the molecular state of 20 μs. There is no systematic shift in the resonance location with temperature or modulation amplitude, but for large amplitude modulations and sufficiently low temperature we observe a nonlinear resonance at $\frac{1}{2}E_b/h$. No other subharmonics are seen. A similar nonlinear response was reported previously [18].

The results of the measurement of binding energy versus B are displayed in Fig. 2(a). In the universal regime [see Fig. 2(b)], where a is much larger than any characteristic length scale of the interaction potential, $E_b = \hbar^2/ma^2$, where m is the atomic mass [2,3]. The solid lines in Fig. 2 show the results of fitting E_b in this universal regime to a, where a is given by the usual Feshbach resonance expression,

$$a = a_{bg}\left(1 - \frac{\Delta}{B - B_\infty}\right), \tag{1}$$

and where a_{bg} is the background scattering length, Δ is the width of the resonance, and B_∞ is the location of the resonance. These three quantities are the only fitted parameters. For $a \gg |a_{bg}|$, the first term in Eq. (1) is small, and the fit is insensitive to a_{bg} and Δ separately. We fix $\Delta = -174$ G (discussed below) and fit to just two free parameters, B_∞ and a_{bg}. The fitted values are given in Table I. In Figs. 2(c) and 2(d), the same data are recast in terms of $\gamma \equiv (mE_b/\hbar^2)^{1/2}$, where for large

TABLE I. Feshbach resonance parameters obtained by fitting γ to Eq. (1) using the various models. There are large uncertainties in a_{bg} and Δ separately, but their product is well defined by the data. The choice of Δ was guided by the coupled-channels calculation. The quoted uncertainty in $a_{bg}\,\Delta$ reflects shot-to-shot variations in the field and fitting uncertainties. The uncertainty in B_∞ is systematic uncertainty in field calibration. Since the range of validity of the nonuniversal models is guaranteed only for $|R_e| \ll a$, data below 725 G are excluded from the fit. The parameters obtained from the fit to Eq. (4) using $R_e(B)$ from Fig. 3 are our recommended values, and are given in bold.

Model	B_∞ (G)	Δ (G)	a_{bg} (units of a_0)	$a_{bg}\,\Delta$ (units of G a_0)
Universal	737.82(12)	−174	−21.0	3660(60)
Simple two-channel	737.68(12)	−174	−19.6	3410(60)
[Eq. (2)] [3]				3410(60)
Complex two-channel [11]	737.73(12)	−174	−20.4	3550(60)
Coupled-channels R_e	**737.69(12)**	**−174**	**−20.0**	**3480(60)**

a, γ versus B is approximately linear, as is shown in Fig. 2(d). We find no significant difference in E_b between a BEC or a thermal gas, to within our uncertainties.

Figure 2 suggests that the universal regime extends down to ∼728 G, or ∼10 G below resonance. Significant discrepancies between the measured E_b and universal theory are observed as the field is decreased further. It is not surprising that the universal regime spans only a small fraction of Δ, since the ^{7}Li resonance is known to be intermediate between closed-channel and open-channel dominated, as the resonance strength parameter $s_{res} \simeq 0.56$ [19] is neither $\ll 1$ nor $\gg 1$ [3,20]. For a more precise determination of a it is desirable to extend the analysis into the nonuniversal regime, where short-range attributes of the potential become appreciable, and where several of the previously identified Efimov features occur [5,7,8]. A simple two-channel approach to correct for finite-range effects, suggested in Ref. [3] and applied to ^{7}Li in Refs. [7,9], is to replace the universal binding energy expression with

$$E_b = \frac{\hbar^2}{m(a - \bar{a} + R^*)^2}, \tag{2}$$

where $\bar{a} = 31\,a_0$ is the mean scattering length [21] (closely related to the van der Waals radius $a_{vdW} = 32.5\,a_0$), and $R^* = \bar{a}/s_{res} = 55\,a_0$ is related to the resonance width [22]. The bound state has predominately open channel character only for $a \gg 4R^*$, which is the expected range of validity of Eq. (2) [3]. The best fit to the data using Eqs. (1) and (2) is plotted in Fig. 2, and the results are presented in Table I.

Although Eq. (2) gives a somewhat better fit to the data than the universal binding energy relation, it clearly fails to represent the entire range of measurements. This is not unexpected as we are comparing the model to data outside its range of validity. We find that higher order corrections to this theory offer little improvement to the overall fit quality [3,23]. The simple two-channel approach [Eq. (2)] represents the effective range of the potential R_e with a single value. Since

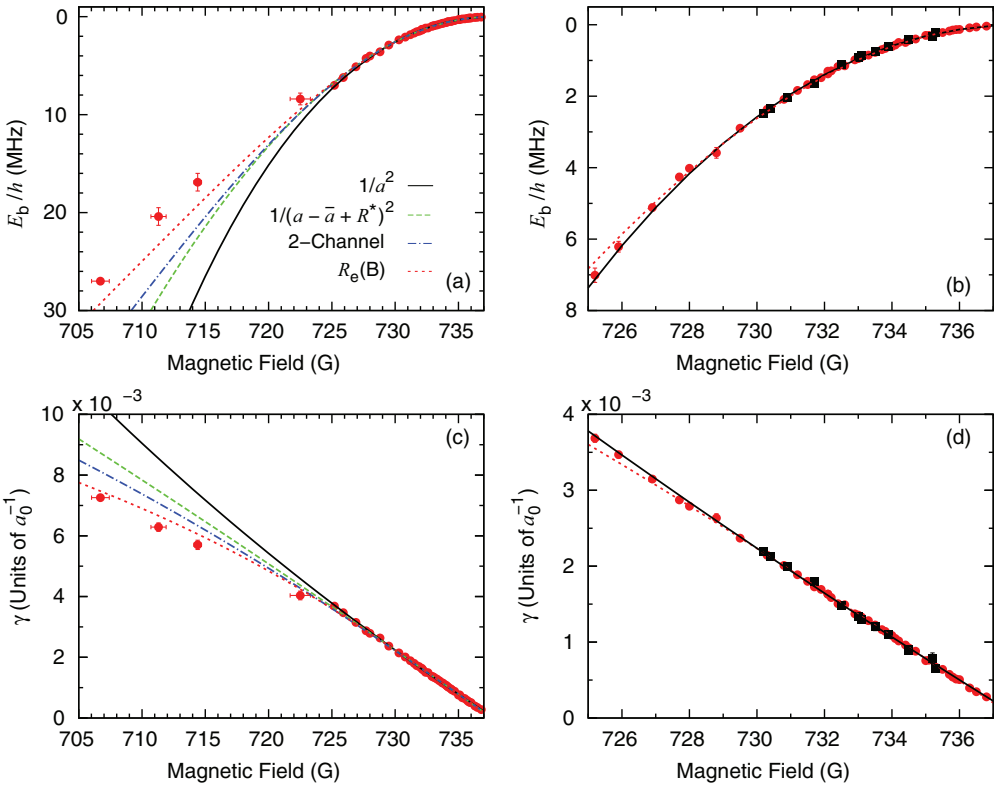

FIG. 2. (Color online) Results of modulation spectroscopy using condensates (red circles) and $\sim 3\,\mu$K thermal clouds (black squares). (a) and (b) E_b vs B; and (c) and (d), the same data plotted as $\gamma \equiv (mE_b/\hbar^2)^{1/2}$ vs B. The vertical error bars correspond to uncertainty in fitting to the binding energy resonances, while the horizontal error bars are the statistical uncertainties due to shot-to-shot variations of the magnetic field. The relatively large error bars below 725 G arise from the broadening of the resonance from the strong modulation required to produce a detectable signal. The lines are fits of the measurements to Eq. (1) using the various models. Solid (black), universal model, $E_b = \hbar^2/ma^2$; dashed (green), simple two-channel model, Eq. (2), with the parameters given in the text; dot-dashed (blue), complex two-channel model given in Ref. [11] [Eq. (26)], again with parameters as given in the text (the two-channel model of Ref. [10] gives similar results); and dotted (red), Eq. (4) using $R_e(B)$ from Fig. 3. The fits exclude data below 725 G, where $a \simeq 250a_0$ is no longer much greater than R^*, and the validity of the nonuniversal corrections becomes questionable. While the nominal fitting parameters are a_{bg}, Δ, and B_∞, Δ is fixed at -174 G. The fits are weighted by the inverse uncertainties. The resulting Feshbach resonance parameters are given in Table I.

the ^{7}Li resonance is not open-channel dominated, however, R_e exhibits considerable field dependence over the width of the resonance. Properly accounting for this field variation should provide a better correction for finite-range effects. In order to obtain $R_e(B)$ we numerically solved the full coupled-channels equations using realistic model potentials for both the singlet (closed channel) and triplet (open channel) potentials of the electronic ground state of Li [24,25]. These potentials have been refined by adjusting parameters, such as the potential depth and the shape of the inner wall, to give quantitative agreement with experimentally known quantities, which are primarily the locations of Feshbach resonances [6,8], zero crossings [6], and the binding energies of the least bound triplet molecule [26]. The scattering length and effective range are determined from the energy dependence of the s-wave phase shift δ_0:

$$k \cot \delta_0(k) = -\frac{1}{a} + \frac{1}{2} R_e k^2 + \cdots, \tag{3}$$

where $\hbar^2 k^2/m = E_{kin}$. Figure 3 shows both a and R_e near the Feshbach resonance at 738 G. There is considerable variation in R_e over the width of the resonance, contrary to the assignment $R_e = -2R^* = -111\,a_0$ [22,28], or $R_e = 2(\bar{a} - R^*) = -49\,a_0$ [3]. In comparison, the coupled-channels calculation gives $R_e(B_\infty) \simeq -6\,a_0$. Given this discrepancy, it is not surprising that Eq. (2) does not describe the data well.

More complex solutions to the two-channel model are given in Refs. [10] and [11]. These complex two-channel models improve upon the simple two-channel model by incorporating a field-dependent effective range. The solution to γ in Ref. [11] [Eq. (26)] is given in terms of R^* and a short-range parameter b, which is related to the van der Waals length and hence, to $\bar{a}$. This short-range parameter is not universal, but rather is model dependent, and is thus unknown *a priori*. One way to estimate b is to require that E_b agrees with Eq. (2) when $1/a = 0$. In this case, $b = \frac{\sqrt{\pi}}{2}\bar{a}$. However, we can use the coupled-channels calculation of R_e to obtain a more informed estimate. For $b = 0.85\sqrt{\pi}\,\bar{a}$, the on-resonance values of R_e calculated from the model of Ref. [11] and from the coupled channels are equal. Using this value for b and the previously specified values of R^* and $\bar{a}$, the best fit to the data is shown in Fig. 2. The expected improvement over the simple model [Eq. (2)] is borne out, as its range of validity (stated as $a \gg a_{vdW}$) is proven to extend to larger detunings from resonance.

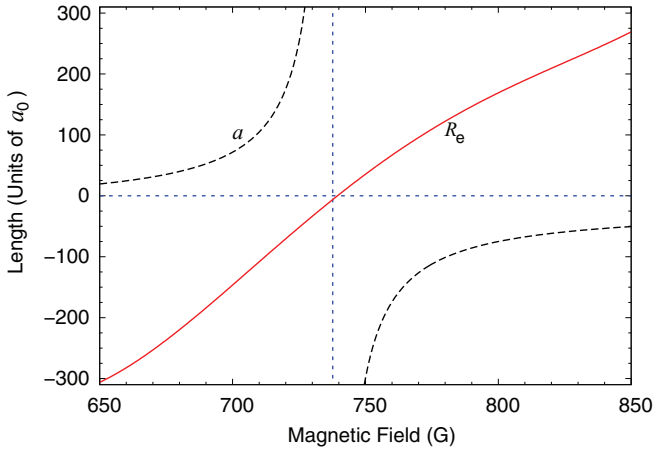

FIG. 3. (Color online) Coupled-channels calculation of a and R_e for the $F = 1, m_F = 1$ Feshbach resonance in ^{7}Li. The horizontal and vertical dashed (blue) lines indicate $a = 0$ and B_∞, respectively. R_e was fit to a polynomial expansion in the scaled field $\beta = (B - 737.7\ \text{G})/\text{G}$ to obtain $R_e(\beta)/a_0 = -6.2 + 3.50\,\beta - 9.2 \times 10^{-3}\,\beta^2 - 6.5 \times 10^{-5}\,\beta^3 + 5.7 \times 10^{-7}\,\beta^4$. This polynomial fit is used to obtain R_e in Eq. (4). Similar calculations for the $F = 1$, $m_F = 0$ [27] and $F = 1, m_F = 1$ [44] resonances have been previously presented. In the latter case, the calculation of R_e agrees well with our results.

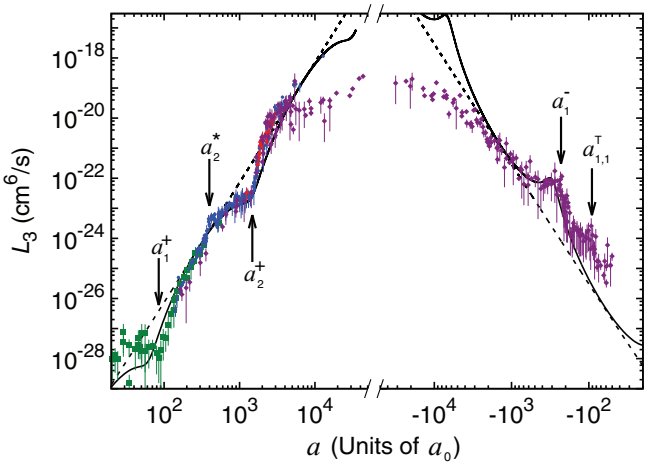

FIG. 4. (Color online) Three-body loss rate coefficient L_3 vs a. The points are values extracted from the measured trap loss, with the green, blue, and red points corresponding to condensates with different trap frequencies, and the purple to a thermal gas ($T \approx 1$–$3\ \mu$K), as reported in Ref. [5]. The solid line shows universal scaling in a, where the positions of the features are determined by the single feature a_2^+. The only additional fitted parameters are the widths $\eta_+ = 0.075$ and $\eta_- = 0.17$, for the $a > 0$ and $a < 0$ sides of the resonance, respectively, and an overall scale factor of 5.5 on the $a > 0$ side of resonance. The need for scaling the universal theory for positive a is unknown. We ascribe the deviation from the universal curve for small, negative a to the presence of the four-body feature $a_{1,1}^T$. The dashed lines are guides to the eye, showing a^4 scaling.

The relation between the binding energy of a weakly bound state, or equivalently γ, and a and R_e is given by $\gamma = 1/a + \frac{1}{2}R_e\gamma^2$ [29]. Although this quadratic equation has two solutions, only the following has the correct asymptotic behavior for $|R_e/a| \ll 1$ [11,22,30]:

$$\gamma = \frac{1}{R_e}\left(1 - \sqrt{1 - \frac{2R_e}{a}}\right). \tag{4}$$

Figure 2 shows the results of fitting the data to Eqs. (1) and (4), using the R_e values from Fig. 3. The agreement between theory and experiment is very good over a much larger range of the measurements than for the other models considered, and we therefore use this fit to define the Feshbach parameters, which are indicated in bold in Table I. As previously mentioned, the data are insufficient to separately extract both a_{bg} and Δ since $a \gg |a_{bg}|$. Given the precise knowledge of the location of the field where $a = 0$, $B_0 = 543.6$, found in our previous work [6], a logical choice would be to fix $\Delta = B_0 - B_\infty = -194.1$ G. The best values of Δ and a_{bg}, however, may vary over the large magnetic field range between the resonance and the zero crossing. We find that $\Delta = -174$ G gives a slightly better agreement to the coupled-channel results for $a > 100\,a_0$, so we adopt this value. We stress, however, that the fit to the data strongly constrains the product $a_{bg}\,\Delta$, but not each parameter separately. The differences in $a(B)$ using Eq. (1) with either value of Δ are less than 2% for $a > 100\,a_0$. A similar procedure was followed in Refs. [7,8]. Our Feshbach parameters agree with Ref. [9], where they find $B_\infty = 737.8(2)$ G, and, although not quite as well, with Ref. [8], which reports $B_\infty = 738.2(4)$ G. Finally, we remark that the model potentials used in the coupled-channels calculation are not *a priori* sufficiently well known to determine $a(B)$ as accurately as the binding energy data. The effective range, on the other hand, varies slowly with B in the region of interest, and we find empirically that its contribution to the uncertainty in γ, via Eq. (4), is small.

We now turn our attention to the three- and four-body Efimov features previously reported in Ref. [5]. Figure 4 shows the measured three-body loss rate coefficient L_3 plotted versus a, where the correspondence between measured values of B is now determined by the new Feshbach parameters given in Table I. While L_3 generally scales as a^4, as indicated by the dashed lines, it is punctuated by several minima and maxima, which arise from the presence of Efimov molecular states. The previously reported [5] Efimov maximum a_2^-, corresponding to the second Efimov trimer, was an error since the upward shift in the resonance position by 0.7 G relative to the previous measurement places this feature in the regime where the loss rates are limited by quantum mechanical unitarity [31–33], where a_2^- cannot be resolved in the data. For the same reason, the effect of the second Efimov tetramer associated with the second trimer ($a_{2,2}^T$) is also not visible in measurements of the four-body loss rate coefficient L_4 (not shown). The fitted locations of the remaining features are given in the second column of Table II, where the caption provides a key to the notation. Not all of the features given in Table II are indicated in Fig. 4, but expanded views of both L_3 and L_4 are found in Ref. [5].

The origins of three of the features in Table II, indicated by square brackets, are uncertain. The feature a_2^* is nominally located at the atom-dimer resonance where the energy of the second Efimov trimer merges with the atom-dimer continuum.

TABLE II. Locations of Efimov features, given in units of a_0, of the three- (L_3) and four-body (L_4) loss coefficients. The experimental values of a are extracted from the measured fields using Eq. (1) with the parameters in bold from Table I. The horizontal lines indicate features that are near the resonance and were not observed. The estimated uncertainties include fitting uncertainties, as well as the uncertainties in the Feshbach parameters. For $a > 0$, a_i^+ denotes the recombination minimum of the i[th] Efimov trimer. The origins of three features, labeled as $[a_2^*]$, $[a_{2,1}^*]$, and $[a_{2,2}^*]$, have not been identified, but roughly correspond to expected locations of atom-dimer and dimer-dimer resonances. For $a < 0$, a_i^- denotes the Efimov resonance where the i[th] trimer merges with the free atom continuum. The remaining features, $a_{i,j}^T$, arise where the j[th] tetramer associated with the i[th] trimer merges with the free atom continuum. The final column gives the predicted locations of the features using universal scaling in a. The universal scaling relations were obtained from the indicated references. The scaling is anchored by the measured location of a_2^+, which, as an input, is denoted by parentheses.

	Feature	Experiment (units of a_0)	Universal scaling in a (units of a_0)
$a > 0$	a_1^+	89(4)	62.57[a]
	a_2^+	1420(100)	(1420)
	$[a_2^*]$	421(20)	317.5[a,b,c]
	$[a_{2,1}^*]$	912(50)	697.3[d]
	$[a_{2,2}^*]$	1914(200)	2154[d]
$a < 0$	a_1^-	−252(10)	−298.1[b]
	a_2^-	—	−6765[b]
	$a_{1,1}^T$	−94(4)	−126.8[e]
	$a_{1,2}^T$	−236(10)	−272.0[e]
	$a_{2,1}^T$	−4060(800)	−2878[e]
	$a_{2,2}^T$	—	−6173[e]

[a]Reference [34].
[b]Reference [35].
[c]Reference [36].
[d]Reference [37].
[e]Reference [38].

Relatively sharp peaks in L_3, located near the expected atom-dimer resonance, were previously reported for ^{39}K [41], and ^{7}Li [5,42]. Since a large dimer fraction is unexpected, a model was developed to explain the presence of enhanced loss even without a large population of dimers [41]. In this model, each dimer produced in a three-body recombination collision shares its binding energy with multiple atoms as it leaves the trap volume due to the enhanced atom-dimer cross section [41]. Recent Monte Carlo calculations, however, conclude that the resulting peak from this avalanche mechanism is too broad and shifted to higher fields to explain the observations [43]. The remaining two features, $a_{2,1}^*$ and $a_{2,2}^*$, are nominally located at dimer-dimer resonances, where the energy of a tetramer merges with the dimer-dimer threshold [39]. Their assignment also remains tentative, since their observation requires a significant and unsubstantiated dimer population.

The third column in Table II gives the predictions of universal scaling. Many of the scaling relations presented in the pioneering papers for the three-body [34] and four-body sectors [39,40] have been replaced by the more precise theoretical determinations cited in Table II. Four significant digits are given to reflect the stated precision of these scaling relations. If the relative positions of all features are universally connected, the position of only one is needed to completely fix the remaining. We choose the recombination minimum of the second trimer, a_2^+, for purpose of comparison, as it is a well-defined feature that occurs at sufficiently large a ($\sim$1400 a_0) to be insensitive to short-range effects, while also being small enough in magnitude to not be hypersensitive to B. While the measured locations are consistent with universal theory at the 20%–30% level, some of the features, in particular a_1^+ and the lowest tetramer $a_{1,1}^T$, occur deep in the nonuniversal regime where $|R_e/a| > 1$. We attempted to correct the universal theory for the effect of finite range using the same strategy applied to the dimer binding energy, that is, by applying universal scaling in γ^{-1} [Eq. (4)] rather than in a. To lowest order, the correction to $1/a$ is $\frac{1}{2}R_e/a^2$. We find that such a replacement improves the agreement with experiment for features on the $a < 0$ side of the resonance, but for $a > 0$ the agreement is actually made worse. We note that an effective field theory for short-range interactions has been developed in which corrections to universal scaling of three-body quantities are computed to $O(R_e)$ and that they have been applied to the $F = 1$, $m_F = 0$ Feshbach resonance in ^{7}Li [44,45]. Effective range corrections have also been used to analyze Efimov features in Cs [46]. It would be interesting to apply the same analysis to the $F = 1, m_F = 1$ resonance in ^{7}Li to compare with the data presented here.

A measure of universality across the Feshbach resonance may be obtained by evaluating the ratio a_2^+/a_1^-. Universal scaling in a implies $a_2^+/a_1^- = -4.76$ [35], whereas experimentally, we find $a_2^+/a_1^- = -5.63$. We disagree with a previous measurement for the $|F = 1, m_F = 1\rangle$ state in ^{7}Li, which found $a_2^+/a_1^- = -4.61$ [8,47]. The Efimov features observed in Refs. [7,8] are not as sharp as those reported here, and this may affect the precision for which the location of a feature is extracted. The width is quantified by the fit parameter η, which is related to the lifetime of the Efimov molecule [34]. For Ref. [8], $\eta_+ = 0.17$ and $\eta_- = 0.25$, corresponding to the $a > 0$ and $a < 0$ sides of resonance, respectively, while we find $\eta_+ = 0.075$ and $\eta_- = 0.17$. These large differences, at least in case of η_+, may indicate that η, and hence the dimer lifetime, has an interesting and unexpected temperature dependence, since the $a > 0$ data in Refs. [7,8] is obtained with a thermal gas, while in our experiment the gas is cooled to nearly a pure Bose condensate.

It was pointed out recently that the location of the first Efimov trimer resonance a_1^-, when scaled by the van der Waals radius a_{vdW}, is remarkably similar for multiple unconnected resonances in the same atom [48], as well as for different atomic species [49]. These observations suggest that there is no need for an additional "three-body parameter" to pin down the absolute positions of the Efimov features, but rather, that this scale is set by short-range two-body physics [49–54]. For the measurements reported here, $-a_1^-/a_{vdW} = 7.8$, which is close to the range of 8–10 reported in most other cases [48,49,53,55].

Quantum mechanical unitarity implies that L_3 is limited for nonzero temperatures, as is evidenced by the purple points in Fig. 4 near the resonance, for which the highest average L_3 is $\sim 8 \times 10^{-20}$ cm^6/s. This value is about 3 times greater than the largest L_3 [33] predicted for a 1-μK thermal gas,

which is the lowest temperature of our thermal data [5]. This discrepancy may indicate a systematic error in measuring L_3 under conditions where the decay rate is comparable to the rate of thermalization.

The determination of the Feshbach parameters for ^{7}Li in the $|F = 1, m_F = 1\rangle$ state by direct measurement of the dimer binding energy is a significant improvement over our previous measurement using condensate size. We have measured the dimer binding energy deep into the nonuniversal regime and find that data are well represented by corrections based on the field-dependent effective range. Using these more precise parameters we find that the overall consistency between the experimentally determined locations of three- and four-body Efimov features and those obtained from universal scaling is in the range of 20%–30%. Since we use the location of only one feature as input, the agreement supports the contention of universal scaling across the Feshbach resonance, but also points to the need for a better understanding of effective range corrections to the Efimov spectrum. The origin of features nominally located at atom-dimer and dimer-dimer resonances remains an open question. A direct measurement of the equilibrium dimer fraction could help to resolve this issue [56].

ACKNOWLEDGMENTS

We thank Eric Braaten, Georg Bruun, Cheng Chin, and Paul Julienne for helpful discussions. Funding was provided by the NSF, ONR, and the Welch Foundation (Grant No. C-1133), and the Texas Norman Hackerman Advanced Resources Program.

[1] V. Efimov, Phys. Lett. B **33**, 563 (1970).
[2] R. A. Duine and H. T. C. Stoof, Phys. Rep. **396**, 115 (2004).
[3] C. Chin, R. Grimm, P. Julienne, and E. Tiesinga, Rev. Mod. Phys. **82**, 1225 (2010).
[4] T. Kraemer, M. Mark, P. Waldburger, J. G. Danzl, C. Chin, B. Engeser, A. D. Lange, K. Pilch, A. Jaakkola, H.-C. Nägerl, and R. Grimm, Nature (London) **440**, 315 (2006).
[5] S. E. Pollack, D. Dries, and R. G. Hulet, Science **326**, 1683 (2009).
[6] S. E. Pollack, D. Dries, M. Junker, Y. P. Chen, T. A. Corcovilos, and R. G. Hulet, Phys. Rev. Lett. **102**, 090402 (2009).
[7] N. Gross, Z. Shotan, S. Kokkelmans, and L. Khaykovich, Phys. Rev. Lett. **105**, 103203 (2010).
[8] N. Gross, Z. Shotan, O. Machtey, S. Kokkelmans, and L. Khaykovich, C. R. Physique **12**, 4 (2011).
[9] N. Navon, S. Piatecki, K. Günter, B. Rem, T. C. Nguyen, F. Chevy, W. Krauth, and C. Salomon, Phys. Rev. Lett. **107**, 135301 (2011) (Supplemental Material).
[10] A. D. Lange, K. Pilch, A. Prantner, F. Ferlaino, B. Engeser, H.-C. Nägerl, R. Grimm, and C. Chin, Phys. Rev. A **79**, 013622 (2009).
[11] L. Pricoupenko and M. Jona-Lasinio, Phys. Rev. A **84**, 062712 (2011).
[12] C. C. Bradley, C. A. Sackett, and R. G. Hulet, Phys. Rev. Lett. **78**, 985 (1997).
[13] S. T. Thompson, E. Hodby, and C. E. Wieman, Phys. Rev. Lett. **95**, 190404 (2005).
[14] T. M. Hanna, T. Köhler, and K. Burnett, Phys. Rev. A **75**, 013606 (2007).
[15] J. P. Gaebler, J. T. Stewart, J. L. Bohn, and D. S. Jin, Phys. Rev. Lett. **98**, 200403 (2007).
[16] S. B. Papp and C. E. Wieman, Phys. Rev. Lett. **97**, 180404 (2006).
[17] J. J. Zirbel, K.-K. Ni, S. Ospelkaus, T. L. Nicholson, M. L. Olsen, P. S. Julienne, C. E. Wieman, J. Ye, and D. S. Jin, Phys. Rev. A **78**, 013416 (2008).
[18] C. Weber, G. Barontini, J. Catani, G. Thalhammer, M. Inguscio, and F. Minardi, Phys. Rev. A **78**, 061601 (2008).
[19] The value of R^* differs from that given in Ref. [3] due the change in Feshbach resonance parameters compared with those given in Ref. [5].
[20] T. Köhler, K. Góral, and P. S. Julienne, Rev. Mod. Phys. **78**, 1311 (2006).
[21] G. F. Gribakin and V. V. Flambaum, Phys. Rev. A **48**, 546 (1993).
[22] D. S. Petrov, Phys. Rev. Lett. **93**, 143201 (2004).
[23] B. Gao, J. Phys. B **37**, 4273 (2004).
[24] E. R. I. Abraham, W. I. McAlexander, J. M. Gerton, R. G. Hulet, R. Côté, and A. Dalgarno, Phys. Rev. A **55**, R3299 (1997).
[25] M. Houbiers, H. T. C. Stoof, W. I. McAlexander, and R. G. Hulet, Phys. Rev. A **57**, R1497 (1998).
[26] E. R. I. Abraham, W. I. McAlexander, C. A. Sackett, and R. G. Hulet, Phys. Rev. Lett. **74**, 1315 (1995).
[27] N. Gross, Z. Shotan, S. Kokkelmans, and L. Khaykovich, Phys. Rev. Lett. **103**, 163202 (2009).
[28] G. M. Bruun, A. D. Jackson, and E. E. Kolomeitsev, Phys. Rev. A **71**, 052713 (2005).
[29] H. Bethe, Phys. Rev. **76**, 38 (1949).
[30] M. Thøgersen, D. V. Fedorov, and A. S. Jensen, Phys. Rev. A **78**, 020501 (2008).
[31] T. Weber, J. Herbig, M. Mark, H.-C. Nägerl, and R. Grimm, Phys. Rev. Lett. **91**, 123201 (2003).
[32] J. P. D'Incao, H. Suno, and B. D. Esry, Phys. Rev. Lett. **93**, 123201 (2004).
[33] B. S. Rem *et al.*, Phys. Rev. Lett. **110**, 163202 (2013).
[34] E. Braaten and H.-W. Hammer, Phys. Rep. **428**, 259 (2006).
[35] K. Helfrich, H.-W. Hammer, and D. S. Petrov, Phys. Rev. A **81**, 042715 (2010).
[36] A. O. Gogolin, C. Mora, and R. Egger, Phys. Rev. Lett. **100**, 140404 (2008).
[37] A. Deltuva, Phys. Rev. A **84**, 022703 (2011).
[38] A. Deltuva, Phys. Rev. A **85**, 012708 (2012).
[39] J. P. D'Incao, J. von Stecher, and C. H. Greene, Phys. Rev. Lett. **103**, 033004 (2009).
[40] J. von Stecher, J. P. D'Incao, and C. H. Greene, Nature Phys. **5**, 417 (2009).
[41] M. Zaccanti, B. Deissler, C. D'Errico, M. Fattori, M. Jona-Lasinio, S. Müller, G. Roati, M. Inguscio, and G. Modugno, Nat. Phys. **5**, 586 (2009).
[42] O. Machtey, Z. Shotan, N. Gross, and L. Khaykovich, Phys. Rev. Lett. **108**, 210406 (2012).
[43] C. Langmack, D. Hudson Smith, and E. Braaten, Phys. Rev. A **86**, 022718 (2012); **87**, 023620 (2012).

[44] C. Ji, D. R. Phillips, and L. Platter, Europhys. Lett. **92**, 13003 (2010).
[45] C. Ji, D. R. Phillips, and L. Platter, Ann. Physics **327**, 1803 (2012).
[46] M. R. Hadizadeh, M. T. Yamashita, L. Tomio, A. Delfino, and T. Frederico, Phys. Rev. A **87**, 013620 (2013).
[47] The notation, a_+ and a_-, in Refs. [7,8] differs from ours: $a_2^+ = 4.764a_+$ and $a_1^- = a_-$. Furthermore, the universal ratio given as $a_+/a_- = 0.96$ in those references should be updated to 1.0, according to Ref. [35].
[48] M. Berninger, A. Zenesini, B. Huang, W. Harm, H.-C. Nägerl, F. Ferlaino, R. Grimm, P. S. Julienne, and J. M. Hutson, Phys. Rev. Lett. **107**, 120401 (2011).
[49] C. Chin, arXiv:1111.1484.
[50] J. Wang, J. P. D'Incao, B. D. Esry, and C. H. Greene, Phys. Rev. Lett. **108**, 263001 (2012).
[51] R. Schmidt, S. P. Rath, and W. Zwerger, Eur. Phys. J. B **85**, 386 (2012).
[52] P. K. Sørensen, D. V. Fedorov, A. S. Jensen, and N. T. Zinner, Phys. Rev. A **86**, 052516 (2012).
[53] S. Knoop, J. S. Borbely, W. Vassen, and S. J. J. M. F. Kokkelmans, Phys. Rev. A **86**, 062705 (2012).
[54] P. Naidon, S. Endo, and M. Ueda, arXiv:1208.3912.
[55] S. Roy, M. Landini, A. Trenkwalder, G. Semeghini, G. Spagnolli, A. Simoni, M. Fattori, M. Inguscio, and G. Modugno, Phys. Rev. Lett. **111**, 053202 (2013).
[56] C. Langmack, D. Hudson Smith, and E. Braaten, Phys. Rev. Lett. **111**, 023003 (2013).